Geoscience Research, ISSN: 0976–9846 & E-ISSN: 0976–9854
Vol. 1, Issue 1, 2010, PP-07-21

Converted P-to-S phase and Moho quality beneath the New Madrid seismic Zone from receiver function studies

Moidaki M.[1]*, Gao S.S.[2], Liu K.H.[2], Abdelsalam M.G.[2], Hogan J.P.[2], Atekwana E.[3]
[1]University of Botswana
[2]Missouri University of Science and Technology
[3]Oklahoma State University, moidaki@mopipi.ub.bw; sgao@mst.edu

Abstract- Receiver functions from numerous teleseismic earthquakes recorded at 26 broadband seismic stations within the New Madrid Seismic Zone (NMSZ) were analyzed to map crustal thickness, Poisson's ratio and Moho thickness within and around the NMSZ. The results show that the average crustal thickness of the stations within the Mississippi embayment is 33.4±0.28 km. The crust thins to about 25.5±1.09 km at OXF and thickens to about 43.3±0.12 km at PLAL. In the Mazatazal Belt, the crust varies from 30.2±0.14 to 53.1±0.29 km thick. However, the crust is thicker at WCI (53.1±0.29 km). There is a dramatic change in crustal thickness between the cratonic stations and stations within the Mississippi embayment. Our results from the Mazatzal belt are comparable to other Proterozoic and Archean shields that include reasonably well determined Moho depths, mostly based on receiver functions. The average crustal thickness for all shields is 39 km, while the average for Proterozoic shields is 40 km, and the average for Achaean shields is 38 km. We observed a dramatic change in crustal thickness from stations with the Mississippi embayment over a very short distance.

Key words: New-Madrid Seismic Zone, receiver functions, Moho sharpness, crustal thickness

1. Introduction

The crustal structure of Middle Proterozoic crust within the New Madrid Seismic Zone (NMSZ) is investigated by using receiver functions to determine the extent of crustal modification. Our understanding of the deep continental crust has improved dramatically over the last decade as a result of detailed seismological studies and numerous studies of lower crustal rocks [1]. However, classification of the crust as mafic or felsic remains the largest uncertainty in determining the crust's overall composition. This is due to (1) the large compositional differences between granulites that occur in terrains, in which felsic rocks dominate and those that are carried as small fragments to the Earth's surface in rapidly ascending magmas (xenoliths, which are dominated by mafic rocks), (2) the very heterogeneous nature of the lower crust as observed in granulite terrains, and (3) the difficulty in determining rock type(s) from average seismic velocities derived from refraction studies. The receiver function analysis method has been used widely in order to understand crustal evolution based on Poisson's ratio, V_p/V_s ratio (Φ) and crustal thickness (H) (Baikal Rift by [2], Arabian plate by [3], Afar rift by [4]). Detailed determination of Φ, H and Moho sharpness (R) have not been done in the NMSZ but earlier geophysical investigations of in NMSZ have indicated a crustal thickness of about 32km, assumed to be caused crustal thinning [5]. The crust in the NMSZ is inferred to have undergone extension mainly in the Cretaceous, but with some Cenozoic episodes [5], and varies in thickness between 30 and 40 km. South of the Mazatzal belt lies the Mississippi embayment which has a sedimentary thickness of ≈5 km, including at least 4–5 km of Cenozoic sediments [5]. There is some evidence from seismic data of crustal thinning beneath the NMSZ [6], and high heat flows are observed in the NMSZ area (about 60mW/m^2). The Mississippi embayment has been studied with reflection and refraction surveys [7]. Sediment thickness within the New Madrid Seismic Zone (NMSZ) from well-log data [8], interpretation of seismic reflection profiles [9], [1] and travel-time differences between the direct and converted waves generated at the base of the sedimentary section [10], [11] have resulted in thicknesses that varies from 405 m to 860 m within the Mississippi by linear interpolation. [12] obtained

Copyright © 2010, Bioinfo Publications

the maximum sedimentary thickness as 640 m and 767 m from 11 of the strong motion stations along a north-south axis in the New Madrid Seismic Zone by means of P and SH wave seismic reflection and refraction techniques. Receiver function analysis of CCM [13] indicates a crust 40 km thick characterized by smooth-velocity gradients down to the Moho. Data from the MOMA array was used previously to investigate crustal thickness and isostasy in the northern Appalachians [14]. Some of the stations from the MOMA array will be incorporated in this study to provide further insights on Poisson's ratio and Moho sharpness in the Proterozoic craton, a region where very few refraction studies exist.

Previous geophysical studies have contributed significantly to our understanding on crustal structure; however, there are still geophysical parameters that need to be addressed in order to fully understand the crustal evolution of the NMSZ. This study will provide new insights on the crustal thickness (H), Poisson's ratio and quantify the sharpness of Moho by stacking teleseismic P-to-S converted waves (PmS) and their multiples (PPmS and PSmS).

2. Geologic setting

The NMSZ, within the Mississippi embayment is a failed Precambrian rift underlying the southern end of the Illinois basin extending from southern Illinois and western Kentucky southwestward to central Arkansas [15], [7]. Reelfoot rift, a southwest-trending aulocogen of late Precambrian-early Paleozoic origin [15],[16] lies beneath the Mississippi embayment. Reactivation of Reelfoot rift structures is believed to be responsible for the current seismicity.

Two distinct regions of deformation are known to overlap, trending from southwest to northeast [6] in the NMSZ. Deep seated Paleozoic normal faults [17] propagate from the northeast. The faults were initiated during the Cambrian with the formation of the Reelfoot rift and have been mapped extensively where exposed in southeastern Illinois. The faults were contractionally reactivated during the late Paleozoic and were again reactivated as normal faults in Mesozoic time [17]. A final recurrence of faulting occurred in the late Tertiary and Pleistocene [18]. The second trend of deformation propagates from the southwest associated with contemporary seismicity in the northeast-striking NMSZ [19].

The major terrains (Fig. **1**) in the study area includes the extensive Northern Rhyolite terrain (1.69–1.78 Ga), the Mazatazal belt (1.61-1.68 Ga) and the granite–rhyolite terrane (1.48–1.45 Ga). The tectonic blocks are interpreted to have been assembled during two main periods of convergent tectonism: 1.74 to 1.70 Ga (Yavapai orogeny) and 1.65 to 1.63 Ga (Mazatzal orogeny) [20]. The Yavapai-Mazatzal province is metamorphosed to greenschist or amphibolite facies. The tectonic units of the Yavapai province are made up of supracrustal rocks of the 1.79 to 1.70 Ga Yavapai Supergroup containing mafic to intermediate volcanic rocks, volcaniclastic, and sedimentary rocks [21]. These are intruded by calc-alkaline batholiths of 1.75 to 1.69 Ga age. The Mazatzal province comprises several blocks: the Mazatzal which are discussed in [22]. Ages in the Mazatzal block range from 1.74 Ga for a gabbro and 1.70 to 1.69 Ga for a suite of volcanic rocks to a 1.65 Ga age for post-tectonic granite, while the Sunflower block contains a 1.64 to 1.63 Ga granitic intrusive suite [23]. The Granite Rhyolite Terrain (1.38-1.48) (Fig. **1**) lies beneath the Paleozoic strata of the Illinois basin and the surrounding region on the basis of outcrops of rhyolite, dacite and related granitic plutons in the St. Francois Mountains of southeastern Missouri and a few scattered basement drill holes located outside the deeper Paleozoic basin areas [24], [5].

3. V_p/V_s ratio and its implications

Poisson's ratio depends on the temperature and pressure and provides constraints on crustal composition than either the P or S wave velocity alone [25]. Laboratory measurements have shown that Poisson's ratio decreases by 0.2% at temperatures in the range of 0^o to 400^o for Co_2SiO_4 olivine and increases by 0.8% to 1.1% for other varieties of olivine. Quartzite show a significant decrease in Φ in the 200^o to 500^o temperature range associated with quartz α-β phase transition [25]. Progressive metamorphism accompanied by systematic changes in plagioclase also contribute to the increase in Poisson's ratio. Granite rocks have low Φ of 1.71 because of high amounts of SiO4. The transition between granite to gabbro is accompanied by decrease in SiO4 and increase in plagioclase content. Mafic and ultramafic intrusions contain gabbro and peridotite or dunite which has originated from magmatic differentiation. A gradual change from gabbro to olivine rich gabbro and dunite lowers Poisson's ratio to approximately 0.26 [25]. Several receiver function-based studies have been conducted using PmS-P and PPmS-P differential travel times [27]. [28] made measurements of Φ and observed that

Precambrian shields have a mean Φ of (1.84 ± 0.06), Archaean-early Proterozoic platforms have an average Φ of (1.75), late Proterozoic have a Φ of 1.78, early Proterozoic have a Φ of 1.76, Mid-late Proterozoic have an average Φ of 1.81, Palaeozoic have an average Φ of 1.73. Cenozoic and Mesozoic crust have lowest Φ of (1.73 ± 0.09) [29] suggesting a relationship between Φ and age of the crust (increase in Φ suggesting an older crust). Studies of the relation between P and S waves velocities seismic refraction data by [29] to infer the composition of the crust in the Grenville and Applachian provinces of North America revealed that the crust exhibits increasing Φ with depth from 1.64 to 1.84 (Grenville with a average Φ of 1.81 and Appalachian with an average Φ of 1.74). The high Φ is an indication of a crust with an average mafic composition. [4] observed Φ values of 1.78 to 2.9 in the Afar region and Main Ethiopian Rift. The high values of Φ were attributed to magma intrusion beneath the crust.

4. Quantification of Moho sharpness (R)

Moho discontinuity is equated with the petrological crust/mantle boundary. From the geophysical point of view, the Moho is defined as the level where the compressional wave velocity sharply increases from normal crustal velocities <7 km/s to typical mantle velocities >7.6 km/s. Mantle rocks are related to olivine dominated systems and the crust mantle boundary is considered as a transition zone where felsic or mafic rocks grade in to peridotite. Therefore the petrologic Moho is characterized by a compositional change whereas the geophysical Moho marks a prominent change of elastic and density properties [30]. The sharpness of the Moho is related to the thickness of the crust-mantle boundary and produces strong PmS and its multiples (a perturbed Moho produces weak PmS and its multiples). The apparent sharpness of the Moho beneath a station is quantified by taking the ratio (R) between the stacking amplitude corresponding to the optimal pair of (H,Φ) and the mean amplitude of the direct P wave on the radial components [31]. R is a function of the angle of incidence and therefore events having an epicentral distance that is ≥70º (Fig. **1**) are weakly affected by variations in the incident angle and suggests that the rays arrive at the station at a near-vertical angle.

The amplitude of the converted phase can be affected by lateral variation in Moho depths [31]. The observed crustal thickness (Fig. **8**) suggests that the Moho in the study area is fairly discontinuous or disturbed, and thus variation in Moho depth is likely to affect the amplitude of the converted phases. Velocity heterogeneities in the crust beneath the area surrounding a station can also affect the PmS amplitudes. The crustal volume traversed by the rays can results to incoherent stacking [31] and consequently reduction in the stacked amplitude of the converted phases. The influence of the topography of velocity interfaces in the crust [31] could also affect the amplitude of the converted phases.

5. Data

We have utilized teleseismic waveforms for receiver function studies from 25 stations: 17 permanent stations and 8 stations from temporary network from 1989 to January 2008. Temporary network stations include 5 stations from Missouri to Massachusetts (MOMA) array (MM14 to MM18) and three stations from Florida to Edmonton (FLED) array (FA07 to FA09). Permanent stations used in this study consists of the following; BLO, CCM, FVM, MIAR, LRAL, MPH, OLIL, OXF, PLAL, PVMO, SIUC, UALR, USIN, UTMT, WCI and WVT. The data was obtained from IRIS data management center. Events used in this study are shown in Fig. **2**. All analyzed phases have steeply dipping incidence angles and sample the upper mantle almost directly beneath the station, providing very good lateral resolution.

6. Method

6.1 Determination of Vp/Vs, H from receiver functions

Converted PmS phases originating from velocity discontinuities have been widely used for studying the crustal structure for several decades e.g. [13], [32]. Receiver functions are calculated by deconvolving the vertical component from the radial and tangential components and are used to isolate and identify PmS converted phases [3]. A Gaussian low pass filter with a corner frequency of 0.5 Hz was applied to all receiver functions. For this study, we have used the H- Φ stacking technique (H = Moho depth and $\Phi = V_p/V_s$ = velocity ratio of V_p and V_s) of [33]. A series of candidate depths Hi in the range from 20 to 70 km in increments of 0.1km and candidate Φj from 1.65 to 2.0 in increments of 0.0025. For each (Hi, Φi) the moveout of PmS, Ppms and PSmS, were calculated using the method of [34], and [31]. The method provides a robust

Copyright © 2010, Bioinfo Publications

Geoscience Research, ISSN: 0976–9846 & E-ISSN: 0976–9854, Vol. 1, Issue 1, 2010

estimate of crustal thickness and Poisson's ratio. Previous studies have shown that there is a strong trade off between depth (H) and velocity ratio (V_p/V_s). The ambiguity introduced by the trade off were reduced by incorporated the later arriving crustal reverberations PpPs and PpSs + PsPs in a stacking procedure whereby the stacking itself transforms the time–domain receiver functions directly to objective function values in H– Φ parameter space [35], [33]. The time delay between the first arriving direct wave and the associated converted phases is a function of depth and velocity structure of the medium [3], [31], [2]. The Moho depth was estimated by using the time difference between the PS_{Moho} phase and the first arrival. Because of the trade off between H and the velocity ratio, incorporating the multiple reflected phases such as PsPs and PpSs+PsPs reduces the trade off significantly [3], [31]. To further enhance the signal to noise ratio and reduce lateral variations, multiple receiver functions are stacked in time domain by using the method developed by [33] that adds the amplitudes of the Ps_{Moho} and multiples at the predicted time by varying H (crustal thickness) and the V_p/V_s ratio. The receiver functions at each of the stations are then stacked using the 'slant stack approach' [33]. The H–Φ stacking algorithm is based on the basis that the weighted stack sum of the receiver function amplitudes should attain its maximum value when H and Φ attain their correct values for a particular crust. The H and Φ values corresponding to the maximum value of the objective function can be determined by performing a grid search through H and Φ parameter space [33]. Events used in this study come from distances of 30^0–100^0 and have magnitudes greater than 5.5. A time-domain iterative deconvolution method [36] was used for computing the receiver functions and to evaluate the quality of the receiver functions. The uncertainty in mean crustal velocity was incorporated into error estimates for H and Φ by specifying a normal distribution of V_p values so that 95% of the values selected fell between 5.9 and 6.5 km s^{-1}, with a mean value of 6.2 km s^{-1}, which is the mean crustal velocity in the NMSZ area. Once values for V_p and the weights were selected, we then used the bootstrap algorithm of [37], together with the H–Φ stacking, to estimate H and Φ with statistical error bounds. While performing the H–Φ stacking, the contribution of each of the receiver functions to the determination of H and Φ was also weighted based on the least squares misfit value of the receiver functions [31]. The H-Φ method requires weights w1, w2, and w3 to be selected, and a value for Vp. More weight is given to the phase that is most easily picked. Given a range of plausible values for Vp (6.3 to 6.8 km/s), crustal thickness can vary by almost 4 km while the Vp/Vs ratio can change by 0.02. Thus, when estimating errors for the H-Φ method, the uncertainty in mean crustal velocity, as well as the sensitivity of our results to variations in weights (w1, w2, w3), must be considered [4]. The procedure of selecting Vp and weights from the distribution described above and then performing the H- Φ stacking with bootstrapping was repeated 10 times. After each time, new average values of H and Φ and their uncertainties were computed. The error estimates in H range from 1.2 km to 5.4 km and the average is 2.9 km. The error estimates for Φ range from 0.03 to 0.2 and the average is 0.12.

6.2 Estimating of Moho sharpness

To estimate the sharpness of the Moho, related to the thickness of the transition zone from the crust to the mantle, the converted P to S (PmS) receiver functions using a constant Φ of 1.73 for all the stations, [38] found that the stacked amplitude of PmS in areas with thick crust is smaller than that in areas with thin crust. They proposed that the Moho beneath thick crust areas was disturbed by Proterozoic events and is thus less sharp. For the Mazatzal belt another possible cause of the observed small stacking amplitudes is that the PmS phases originated from a deeper Moho are stacked less coherently, because the Φ values in this area are significantly larger than 1.73, which was the value used for the stacking by [38]. A sharp Moho produces strong PmS and its multiples. To quantify the apparent sharpness of the Moho beneath a station, the ratio amplitude R, the ratio between the stacking amplitude corresponding to the optimal pair of (H, Φ) and the mean amplitude of the direct P wave on the radial components. R is a function of the angle of incidence, therefore events with an epicentral distance that is greater than 70^o (Fig. **3**) suggests that most of the rays arrive at the station at a near-vertical angle, and thus are weakly affected by variations in the incident angle. In addition, the resulting distribution of R shows a high level of spatial consistency (see Fig. **9**) and correspondence with geologic provinces (Fig. **1**), suggesting that the resulting R values indeed reflect the sharpness of the Moho.

7. Results

The approach applied in this study makes use of a simple stack of receiver functions and the arrival times of the Ps and PpPs phases. Observations of H, R, and Φ were obtained at most of the 25 stations (Table 1). The receiver functions were categorized in four groups based on the quality of the H- Φ plots. Those in category A display a clear defined single peak in the H- Φ plots, and therefore both H and Φ can be determined with high confidence. Category B stations show clear PmS but not PPmS or PSmS. Thus an optimal pair of (H, Φ) cannot be determined. For these stations, an estimate of the crustal thickness (Hn) was obtained by using a global average Φ of 1.73. Category C involves stations in which none of the three Moho phases used in the study can be clearly observed, and therefore neither H nor Φ can be determined. A larger departure of the real Φ beneath a station from 1.73 results in greater error in the estimated thickness (Hn). For these stations, the resulting maximum stacking amplitude (R) provides unrealistic Moho amplitudes values. For the entire study area, the resulting Φ values range from 1.752 to 1.90, with a mean of 1.84, and the crustal thickness ranges from 25.1 km to 53.1 km, with a mean of 44.18 km. The R values have a mean of 0.122 with a range of 0.034-0.348. The study area is divided in three zones (Zone 1: stations within the Mississippi embayment, Zone 2: Stations on the Craton and Zone 3: stations of the orogenic belts).

7.1 Stations within the Mississippi Embayment (zone 1)

7.1.1 H- Φ stacking results

Stations within the Mississippi embayment (Fig. **1**) are underlain by up ≈5 km of sediments. These sediment deposits are unconsolidated and poorly consolidated, age ranges from late Cretaceous to present, and uncomformably overlay Paleozoic carbonate and clastic rocks [39]. Radial receiver functions were stacked over a time window at -4 to 48 s for all stations in Mississippi embayment. The direct P-wave arrives at 1 s to 2 s with PmS phases arriving at 3 s to 6 s. The P phase for most of the stations within the Mississippi embayment manifest apparent offsets from zero time due to the effects of thick sedimentary layers. Such lags are apparent at MPH, UTMT, PVMO and OXF. For most stations, PmS phases arrive at roughly 3-7 s and the Moho reverberations PpPs range from 16 to 28 s. There is a strong similarity between PmS phases and Moho reverberations from adjacent stations, e.g. UTMT and PVMO, with clear differences in the direct arrival of the P-wave at WVT and PLAL. The crustal thickness beneath these stations ranges from 29±0.15 km (UTMT) to 46.3±0.12 km at PLAL. The values of Φ ranges from 1.749 at UTMT to 1.995* at WVT (Fig. **4**). The ratio values direct P and PmS ranges from 0.038 (PLAL) to 0.38 (UTMT). Both H and Φ are spatially consistent, as indicated by the small STD (Table 1).

7.1.2 Stations on the Craton (zone 2)

The stations on the Mazatzal Belt (1.61-1.68 Ga), a NE trending Precambrian belt consists of permanent and temporary stations (MM14 to MM18) from the MOMA array. The stations were previously studied by [14]. Stations within this group show well defined measurable crustal thickness from receiver functions (Fig. **1** and Table 1). P to S conversions at the Moho show strong amplitudes due to the Moho's large velocity contrast and are clearly visible even on individual receiver functions. Assuming a conversion depth of 40 km, Moho conversion points for events recorded at one station sample a relatively small area around the station. Radial receiver functions were stacked together for each station. The strong phases at 0 s with large amplitudes are direct P wave arrivals. Certain P phases manifest apparent offsets from zero time due to the effects of thick sedimentary layers. Such lags are observed at MM16 to MM17 and BLO that are located in the Illinois basin. For most stations, Pms phases arrive at roughly 4-6 s and the Moho reverberations PpPs range from 15 to 28 s. PmS phases and Moho reverberations are similar for certain groups of adjacent stations, for instance, MM16–CCM, but clear differences exist across the array with the PcS phase being observed at BLO and CCM (Fig. **3**). The receiver function at UALR displays a significantly earlier PmS phase and Moho reverberation than those at other stations, suggesting a much shallower Moho. The phases at roughly 7 s on the stacks for MM17 seem too late for Moho conversions, and they may include interference between PmS and reverberations from discontinuities in the shallow crust which is shown by a strong PcS phase on stacked receiver function. The Moho reverberations at MM17 are similar to reverberations at adjacent stations. Cratonic stations are located on the mid-continent platform (Paleozoic sediment rest on Precambrian basement). The crustal thickness

Copyright © 2010, Bioinfo Publications

Geoscience Research, ISSN: 0976–9846 & E-ISSN: 0976–9854, Vol. 1, Issue 1, 2010

beneath the Proterozoic NMSZ at WCI is among the thickest (53.1km), with values of Φ (1.744) and low values of R (0.083) measurements. Station CCM was previously studied by [46] and obtained a crustal thickness of about 40 km which is lower than to 47.2 km obtained in this study (Fig. **5** and Table 1).

7.1.3 Orogenic belts stations (zone 3)

Stations in this category are characterized by clear PmS arrival with the direct P-wave at an offset of <1 s. These stations show a well pronounced PcS phase due sub-crustal interferences. The Moho reverberations arrive between 16 and 28 s. These stations are characterized by thick crust (42-52 km) and Φ values between 1.789 to 1.915 (Table 1 and Fig. **7**). The R values observed at these stations is lower than those observed at stations within the Mississippi embayment (Fig. **9**). The averaged H, Vp/Vs and R values are shown in table 1. The large contrast in crustal thickness (H) and Moho sharpness (R) between the MIAR and LRAL stations suggests that the crust has different characteristics.

8. Discussion

8.1 Spatial distribution of Φ

The results presented in this paper are perhaps the most precise quantitative seismic measurements of crustal and Moho properties ever obtained for NMSZ area. We present quantitative results suggesting that the crust beneath the region of study in the North American craton is more mafic in composition. The Vp/Vs (Φ) distribution is remarkably coherent throughout the Mazatzal belt and orogenic belts with lower values observed at BLO and OLIL. Stations within the Mississippi embayment have variable Vp/Vs rations with lower values at PVMO and UTMT. The Ouachita (station MIAR) – Appalachian (stations FA07 and LRAL) Orogens show values of Φ that are similar to but more spatially consistent than the cratons. The observed Φ values have no obvious relationship with either crustal thickness or the age of the surface rocks. The regions of thicker crust (Mazatzal belt and orogenic belt stations) show a wide range of Φ values. The thinnest crust in the Mississippi embayment (at UTMT and PVMO) possesses the smallest Φ. There is no obvious age relationship to Φ, as there is no significant difference in Φ between on-craton and off-craton regions. The most prominent characteristic of the data set is that the highest values for Φ are found on cratonic stations. [28] suggest increasing Φ with age. Our results are clearly consistent with this observation. [28] obtained an average value of 1.81 ± 0.04 for shields and platforms, while [40] obtained an average value of 1.76 ±0.01. The mean Φ value (1.84) obtained in this study suggest that mafic layer successfully accounts for both the thickness and V_p/V_s ratio variations between NMSZ region and the rest of the study area.

8.2 Composition of the NMSZ and Vp/Vs ratio

Petrological studies suggest that the upper continental crust is felsic [41]. The mineralogy is the most important factor influencing Vp/Vs or Poisson's ratio with the abundance of quartz and plagioclase feldspars having a dominant effect on common rocks. Granitic rocks have a Poisson's ratio of 0.24 while intermediate composition rocks (e.g. diorite) have values around 0.27 and mafic rocks (e.g. gabbro) about 0.30 [25]. Based on the classification of [42], rocks with a Φ of 1.76 or smaller are considered felsic, between 1.76 and 1.81 as intermediate, and larger than 1.81 as mafic. This classification was used with our estimate of Φ to constrain the crustal composition of NMSZ. Proterozoic crust has been found to have V_p/V_s ratio of 1.78±0.06 [31]. The observed high values of Φ (1.82) of the Mazatzal belt are a result of crustal modification by tectonic activity. The variability in Moho depth beneath the stations reflects differences in the amount of crustal modification. The high Vp/Vs ratio within the Mazatzal belt indicates the presence of mafic crust. Our average value of 1.84 is thus significantly higher and corresponds to a low SiO_2 content.

8.3 Effects of sediments on receiver functions

The thick low-velocity sedimentary structure significantly affects the crustal Ps image beneath the basin area. In addition, the Moho can hardly be traced continuously beneath the basin area mostly due to the substantial interference of the strong sediment reverberations with the Moho Ps signal [43]. The Moho can be coherently identified at UTMT, ranging from ~29 km at the to ~46.3 km at PLAL. The shallow Moho depth within the Mississippi embayment is a result thinned continental crust due Precambrian tectonic activity. The thinner crust with small thickness variations in the basin area suggest that the crust might have been thinned at the same time

the lithosphere was thinned during late Mesozoic to Cenozoic. This result is consistent with the present-day high surface heat flow of the region [6].

8.4 Moho sharpness beneath the NMSZ

The Moho is remarkably flat beneath the stations outside the Mississippi embayment and less sharp. Our analysis of crustal parameters employs a methodology that makes use of Moho converted phases and crustal reverberations to determine precisely the Vp/Vs ratio (Poisson's ratio). Moho reverberation phases are the weak signals reflected by Earth's surface and the Moho that occur in the coda of the direct P-wave arrival. Although the P to S converted wave from the Moho, the dominant phase on typical receiver function records [13], [44] is widely used to determine Moho depth, the later reverberation phases are rarely used, because poor signal to noise ratio and the difficulty of obtaining reliable waveforms or even of detecting them at all. The sharpness and the topographic relief on the Moho are quantitatively constrained to a high level of accuracy. These findings provide critical constraints on the mechanisms of crustal formation and evolution in NMSZ and the surrounding area. Additional insights that emerge from this study as to the structure and morphology of the Moho beneath the seismic stations is that within stations on the craton, the Moho is perturbed and well preserved for stations within the Mississippi embayment. There is a dramatic change in Moho quality between station within the Mississippi embayment and station off the rift. The other constraint is that the Moho is extremely flat, with a maximum variation in crustal thickness of ≈2 km over the study area. The Moho transition thickness and the variation in crustal thickness are therefore maximum estimates. The observed sharpness and flatness of the Moho have fundamental implications for crustal formation and evolution in the Archean crust. The assembly history of North American crust is complex, spanning nearly 1 billion years of geologic time [5]. Although details of crustal aggregation are still unclear, models typically involve extensive collisional accretion of island arcs and micro-continental blocks to form nuclear continental masses. Such accretionary processes may be expected to produce a complicated mosaic of varying Moho structures and diverse crustal lithologies. On the other hand, relatively flat Moho structures have been found to be preserved over areas of significant extent in some Phanerozoic accretionary terranes in western Canada [45], so it remains possible that the Moho structures observed today are simply those preserved from the time of crustal formation. An alternative and more plausible explanation of our observations is that the North American crust was assembled by accretionary tectonics, but that the flat and perturbed Moho was achieved in a later stage of crustal evolution. This explanation implicitly requires that a large volume of the crust has been re-worked on a regional scale since its formation.

9. Conclusion

The Mazatzal belt within the North American craton is characterized by high values of Φ, suggesting a mafic upper and lower crust. The largest Φ values are spatially distributed within the North American craton, and are most likely due to the intrusion of basalt into the crust. The addition of basaltic material successfully explains the thicker crust, higher Φ, as well as the diffuse character of the Moho in this area. We suggest that mafic addition is a dominant process in the modification of crustal composition. Collisional zones, Ouachita – Appalachian, have values of Φ that are not significantly different from surrounding regions. Φ values observed within the Mississippi embayment are highly variable probably to the effects of sediment on receiver functions. Because such collisions are expected, through erosion of the top layer, to make the crust more mafic (if the lower crust is more mafic than the upper crust), we infer that the upper and lower crust are similar in composition in this region.

10. Acknowledgment

The data set used in the study was obtained from IRIS DMS.

11. References

[1] Rudnick, R.L., and Fountain D. M. (1995). Nature and composition of the continental crust: A lower crustal perspective, Reviews of Geophysics, 33, 3, 267-309.

[2] Gao, S.S., K.H. Liu, and C. Chen (2004). Significant crustal thinning beneath the Baikal rift zone: New constraints from receiver function analysis. Geophysical Research Letters, VOL. 31, L20610, doi:10.1029/2004GL020813.

[3] Al-Damegh, K., E. Sanvol, and M. Barazangi (2005). Crustal structure of the Arabian plate: New constraints from the analysis of teleseismic receiver

Copyright © 2010, Bioinfo Publications

functions, Earth and Planet. Sci. Lett., 231, 177-196.

[4] Dugda, M.T., A.A. Nyblade, J. Julia, C.A. Langston, C.J. Ammon, and S. Simuya (2005). Crustal structure on Ethiopia and Kenya from Receiver function analysis: Implications for rift development in eastern Africa. Journal of Geophysical Research, Vol 11-, B01303, doi 10.1029/2004JB003065.

[5] Van Schmus, W.R., and W.J. Hinze (1985). The Midcontinent Rift System. Ann. Rev. Earth Planet. Sci., 13: 345-383.

[6] Bexfield, C.E., J.H. McBride, A.J.M. Pugin, D. Ravat, S. Biswas, W.J. Nelson, T.H. Larson, S.L. Sargent, M.A. Fillerup, B.E. Tingey, L. Wald, M.L. Northcott, J.V. South, M.S. Okure, M.R. Chandler (2006). Integration of P- and SH-wave high-resolution seismic reflection and micro-gravity techniques to improve interpretation of shallow subsurface structure: New Madrid seismic zone, Tectonophysics 420, 5–21.

[7] Braile, L. W. (1989). Crustal structure of the continental interior, in Geophysical framework of the continental United States, edited by L. C. Pakiser and W. D. Mooney, Memoirs of the Geol. Soc. of America, 172, 285-315, Boulder, Colo.

[8] Dorman, J., and R. Smalley (1994). Low-frequency seismic surface waves in the Upper Mississippi Embayment, Seism. Res. Lett., 65(2):137-148.

[9] Mooney, W. D., M. C. Andrews, A. Ginzburg, D. A. Peters and R. M. Hamilton (1983). Crustal structure of the northern Mississippi embayment and a comparison with other continental rift zones, Tectonophysics, 94, 327-348.

[10] Hough, S. E. (1990).Constraining sediment thickness in the San Francisco Bay area using observed resonances and Ps conversions, Geophys. Res. Lett., 17, 1469-1472.

[11] Chen, K. C., J. M. Chiu, and Y. T. Yang (1996). Shear-wave velocity of the sedimentary Basin in the upper Mississippi Embayment using S _to P converted waves, Bull. Seis. Soc. Am., 86, 848-856.

[12] Street, R., E. Woolery, Z. Wang, and J. Harris (1995). A short note on shear-wave velocities and other site conditions at selected strong-motion stations in the New-Madrid seismic zone, Seis. Res. Lett., 66, 56-63, 1995.

[13] Langston, C. A. (1979). Structure under Mount Ranier, Washington, inferred from teleseismic body waves, J. Geophys. Res., 84, 4749-4762.

[14] Lie, A., D.W. Forsyth, K.M. Fisher (2003). Shear velocity structure and azimuthal anisotropy beneath eastern North America from Rayleigh wave inversion. J. Geophys. Res. 108 (B8) (Art. No. 2362).

[15] Ervin, C. P., and L. D. McGinnis (1975). Reelfoot rift: Reactivated precursor to the Mississippi embayment, Geological Society of America Bulletin, **86**, 1287-1296.

[16] Braile, L. W., G. R. Keller, W. J. Hinze, and E. G. Lidiak (1982). An ancient rift complex and its relation to contemporary seismicity in the New Madrid seismic zone, Tectonics, **1**, 225-237.

[17] Kolata, D.R., and W.J. Nelson (1991). Tectonic history of the Illinois Basin: American Association of Petroleum Geologists, Memoir 51, p. 263–285.

[18] Nelson, W.J., F.B. Denny, L.R. Follmer, J.M. Masters (1999). Quaternary grabens in southernmost Illinois: deformation near an active intraplate seismic zone. Tectonophysics 305, 381– 397.

[19] Chiu, J.M., A.C. Johnston, Y.T. Yang, (1992). Imaging the active faults of the central New Madrid seismic zone using PANDA array data. Seismological Research Letters 63, 375– 393.

[20] Van Schmus, W.R., D.A. Schneider, D.K. Holm, S. Dodson, B.K. Nelson (2007). New insights into the southern margin of the Archean–Proterozoic boundary in the north-central United States based on U–Pb, Sm–Nd, and Ar–Ar geochronology, recambrian Research 157,80–105.

[21] Eisele, J., and C.E. Isachsen (2001). Crustal growth in southern Arizona: U-Pb geochronologic and Sm-Nd isotopic evidence for addition of the Paleoproterozoic Cochise block to the Mazatzal Province: American Journal of Sciences, v. 301, p. 773–797.

[22] Holm, D.K., D.A. Schneider, S. Rose, C. Mancuso, M. McKenzie, K.A. Foland, K.V. Hodges (2007). Proterozoic metamorphism and cooling in the southern Lake Superior region, North America and its bearing on crustal

evolution, Precambrian Research 157, 106–126

[23] Karlstrom, K.E., and S.A. Bowring (1988). Early Proterozoic assembly of tectonostratigraphic terranes in southwestern North America: The Journal of Geology, v. 96, 561–576.

[24] Denison, R. E., R.B. Koepnick, W.H. Burke, E.A. Hetherington, and A. Fletcher (1984). Construction of the Mississippian, Pennsylvanian and Permian seawater 87Sr/86Sr curve. Chem. Geol. 112:145–167.

[25] Christensen, N. I. (1996). Poisson's ratio and crustal seismology, J. Geophys. Res., 101, 3139– 3156.

[26] Clarke, T. J., and P. G. Silver (1991). A procedure for the systematic interpretation of body wave seismograms. 1. Application to Moho depth and crustal properties, Geophys. J. Int., 104, 41– 72.

[27] Zandt, G., and C. J. Ammon (1995). Continental-crust composition constrained by measurements of crustal Poisson's ratio, Nature, 374, 152–154.

[28] Musacchio G., W.D. Mooney, J.H. Luetgert, and N.I. Cristensen (1997). Composition of the crust in the Grenville and Appalachian Provinces of North America inferred from Vp/Vs ratios, Journal of Geophysical Research, Vol 102, NO B7, Pahes 15,225-15,241.

[29] Scheuber, E., P. Giese, F.Schilling, M. Schmitz, and P. Wigger (1999). Crustal thickening in the Central Andes and the different natures of the Moho discontinuity. J. South American Earth Sci., 12, 201-220.

[30] Nair, K.S., S.S. Gao, K.H. Liu, and P.G. Silver (2006). Southern African crustal evolution and composition from receiver function studies. Journal of geophysical research, vol.111, B02304, doi:10.1029/2005JB003802.

[31] Owens, T. J., G. Zandt and S. R. Taylor (1984). Seismic evidence for an ancient rift beneath the Cumberland Plateau, Tennessee: A detailed analysis of broadband teleseismic P waveforms, J. Geophys. Res., 89, 7783-7795.

[32] Zhu, L. P., and H. Kanamori (2000). Moho depth variation in southern California from teleseismic receiver functions, J. Geophys. Res., 105, 2969– 2980.

[33] Dueker K.G., and A.F. Sheehan (1993). Mantle discontinuity structure beneath Colorado Rocky Mountains and High Plains, J. Geophys. Res., 103, 7153-7169.

[34] Ammon, C. J., G. E. Randall, and G. Zandt (1990). On the non-uniqueness of receiver function inversions, J. Geophys. Res., 95, 15,303– 15,318.

[35] Ligorria, J. P., and C. Ammon (1999). Iterative deconvolution and receiverfunction estimation, Bull. Seismol. Soc. Am., 89, 1395–1400.

[36] Efron, B., and R. Tibshirani (1991). Bootstrap methods for standard errors, confidence intervals, and other measures of statistical accuracy, Stat. Sci., 1, 54– 77.

[37] Nguuri, T. K., J. Gore, D. E. James, S. J. Webb, and Kaapvaal Seismic Group (2001). Crustal structure beneath southern Africa and its implications for the formation and evolution of the Kaapvaal and Zimbabwe cratons, Geophys. Res. Lett., 28, 2501– 2504.

[38] Andrews, M. C., W. D. Mooney, and R. P. Meyer (1985). The relocation of microearthquakes in the northern Mississippi embayment, J. Geophys. Res. 90, 10223-10236.

[39] Chevrot, S., and R. D. van der Hilst (2000). The Poisson ratio of the Australian crust: Geological and geophysical implications, Earth Planet. Sci. Lett., 183, 121–132.

[40] Christensen, N. I., and W. D. Mooney (1995). Seismic velocity structure and composition of the continental crust: A global view, J. Geophys. Res., 100, 9761–9788.

[41] Ferris, A., G. A. Abers, B. Zelt, B. Taylor, and S. Roecker (2006). Crustal structure across the transition from rifting to spreading: the Woodlark rift system of Papua New Guinea Geophys. J. Int. 166, 622–634 doi: 10.1111/j.1365-246X.2006.02970.x.

[42] Zheng, T.Y., L. Chen, L. Zhao, W.W Xu, and R.X. Zhu (2006). Crust–mantle structure difference across the gravity gradient zone in North China Craton: seismic image of the thinned continental crust. Phys. Earth Planet. Int. 159, 43–58

[43] Kind, R., G.L. Kosarev, and N.V. Petersen (1995). Receiver function at the stations of the German Regional Seismic Network (GRSN), Geophys. J. Int. 121, 191-202.

Copyright © 2010, Bioinfo Publications

Geoscience Research, ISSN: 0976–9846 & E-ISSN: 0976–9854, Vol. 1, Issue 1, 2010

[44] Cook, F.A., (1995). The reflection Moho beneath the southern Canadian Cordillera, Can. J. Earth Sci. 32,1520-1530.

[45] Langston, A.C. (1994). An integrated study of crustal Structure and Regional wave propagation for Southern Missiouri, Bull. Seis. Soc. Am., 84, 105-118.

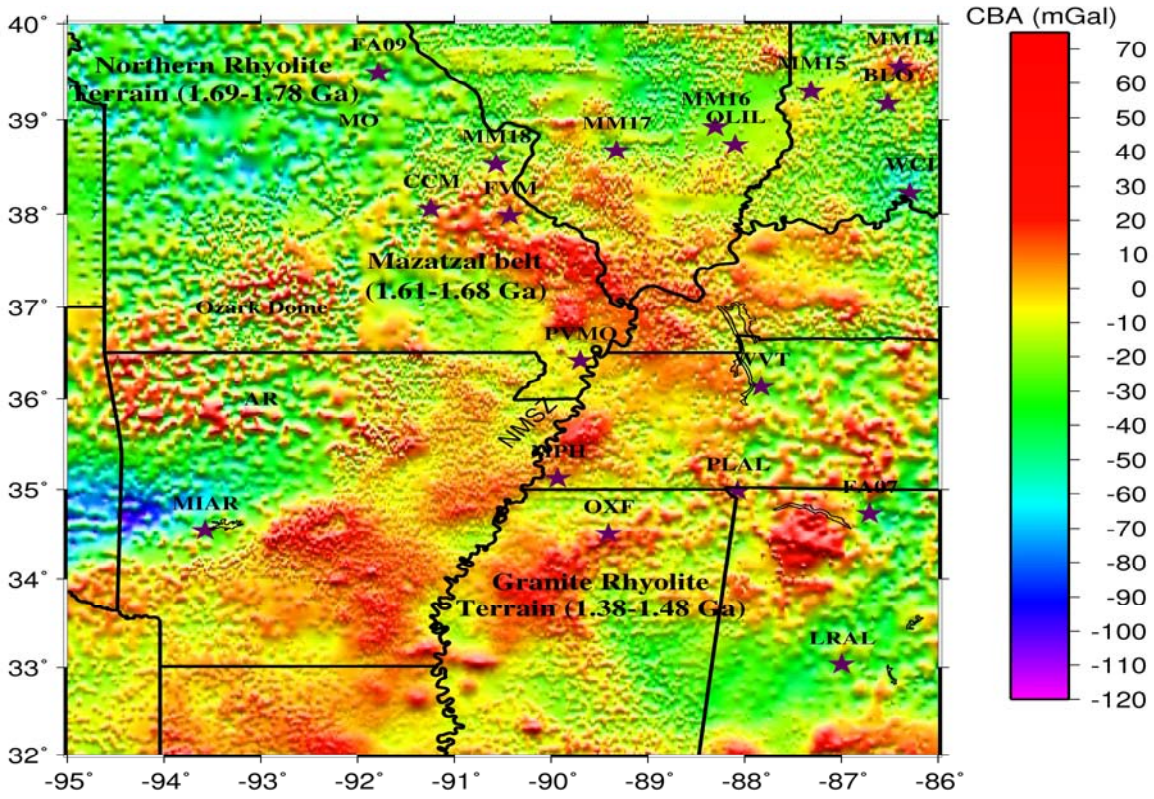

Fig. 1- Complete Bouguer anomaly of the NMSZ showing seismic stations used for receiver function studies. The purple stars represent the location of broadband stations (Gravity data was obtained from PACES: Pan-American Center for Earth and Environmental Studies).

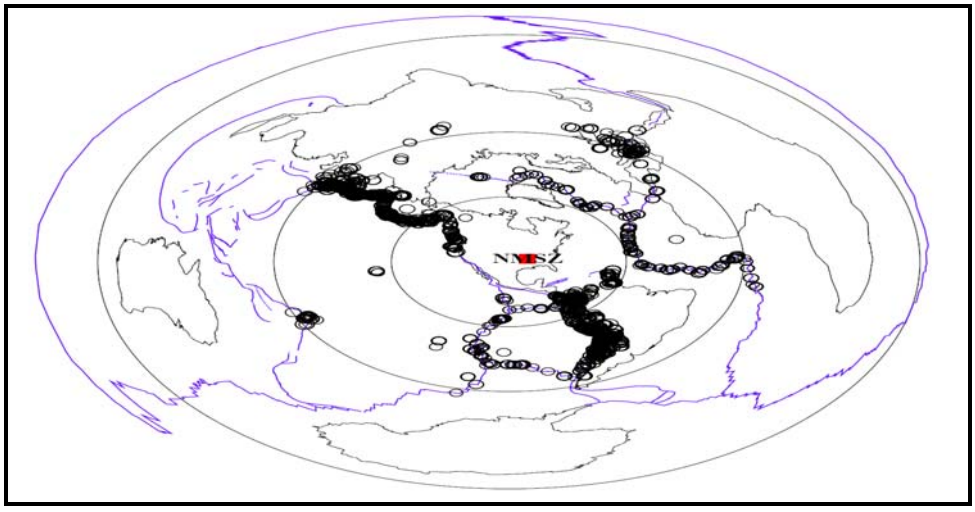

Fig. 2-Locations of high quality events used for receiver function analysis used in this study.

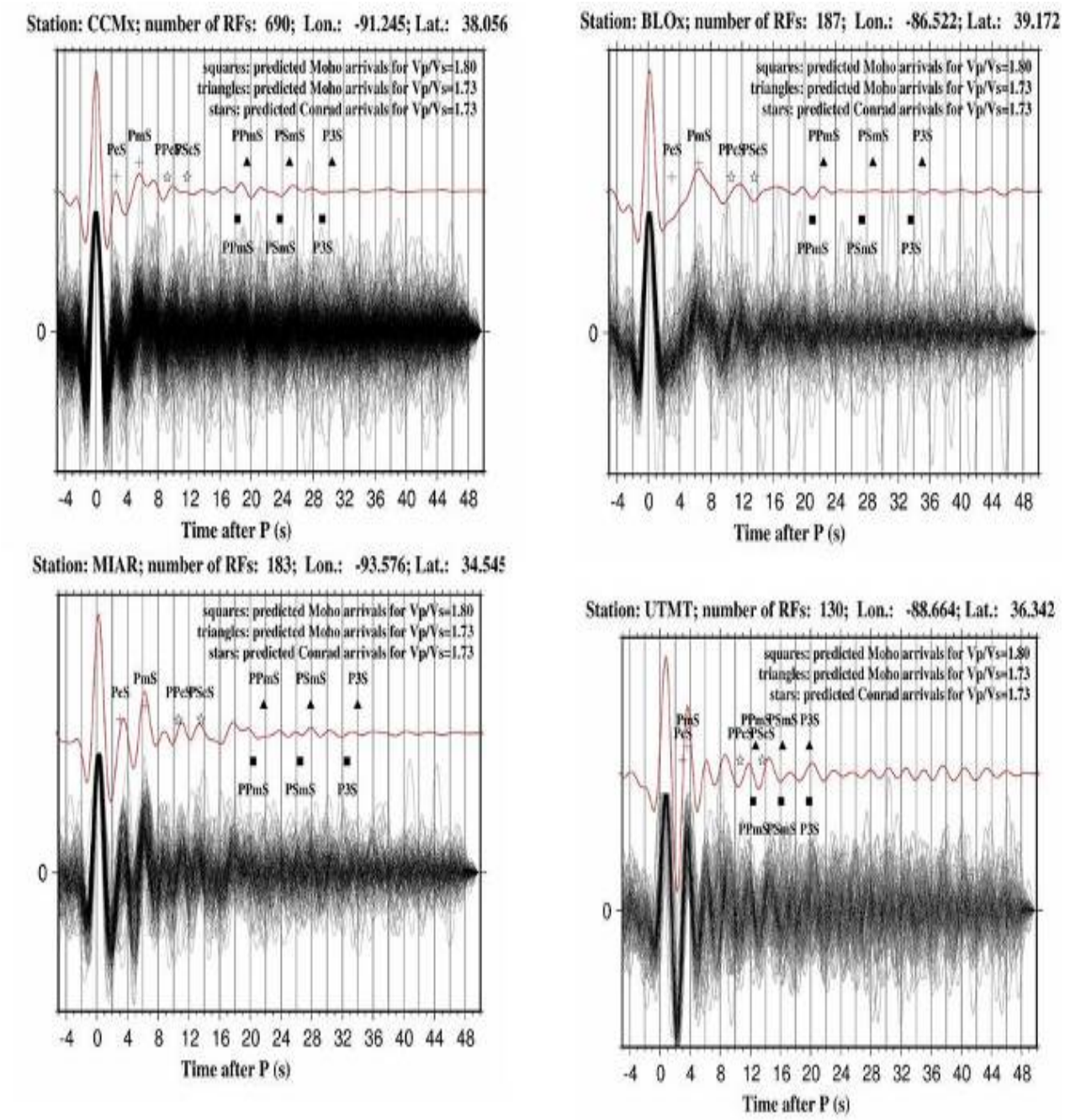

Fig. 3-Stacked receiver functions in time domain for station CCM, BLO, MIAR and UTMT. The PmS phase is well pronounced for all the stations with MIAR showing a strong PcS phase suggesting a subcrustal interface before the Moho. The single trace at the top of the individual receiver functions is the result of simple time domain summation of individual traces. Triangles are theoretical arrival times for PPmS and PSmS calculated using equations (2) and (3) by taking p=5.0s/deg, V_p=6.5 km/s and Φ=1.73.The time difference between the PmS and the direct arrival is approximately 5sec (~40km of crustal thickness).

Copyright © 2010, Bioinfo Publications

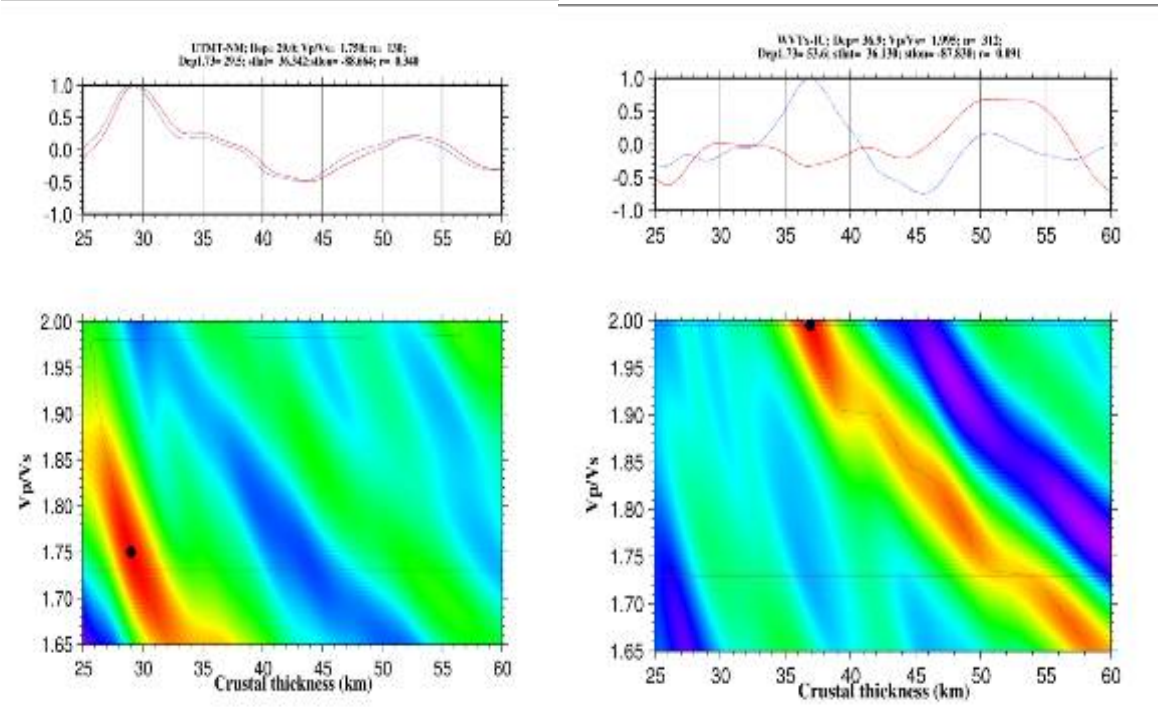

Fig. 4- H-Φ plots for UTMT and WVT. The red line shows the stacking amplitude for Φ=1.73. The blue line was obtained by using the optimal Φ. The resulting thickness, Φ, and the crustal thickness when Φ=1.73 (denoted as Depth1.73) are shown on the top panels.

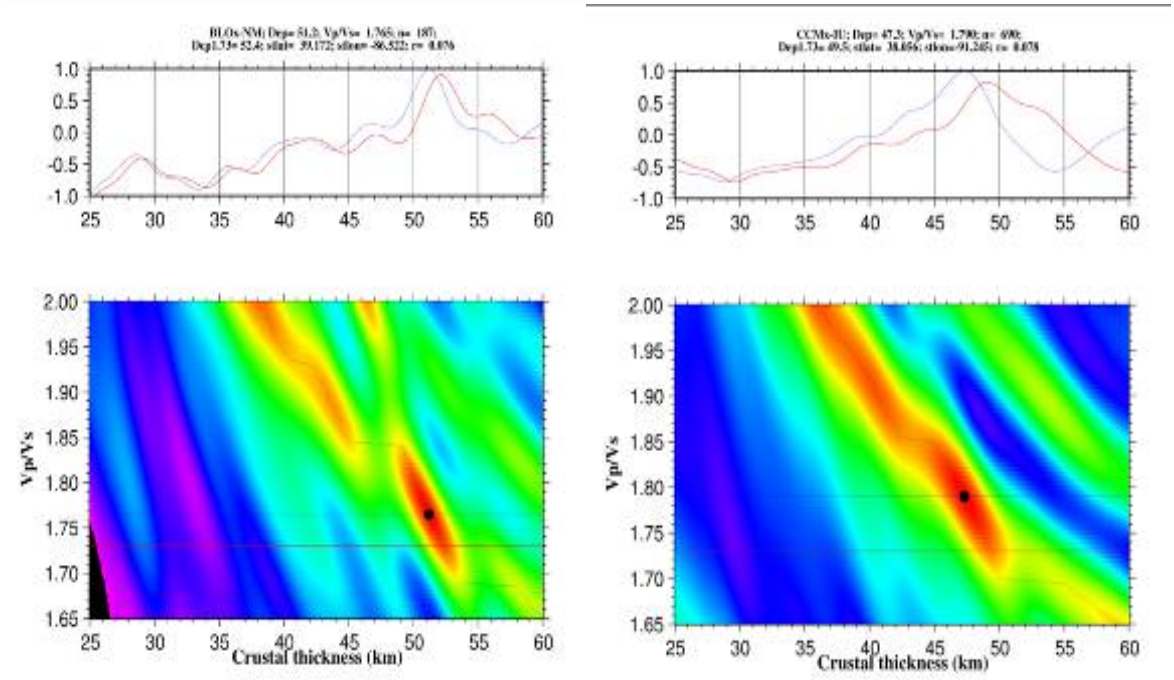

Fig. 5-H-Φ plots for BLO and CCM. The red line shows the stacking amplitude for Φ=1.73. The blue line was obtained by using the optimal Φ. The resulting thickness, Φ, and the crustal thickness when Φ=1.73 (denoted as Depth1.73) are shown on the top panels.

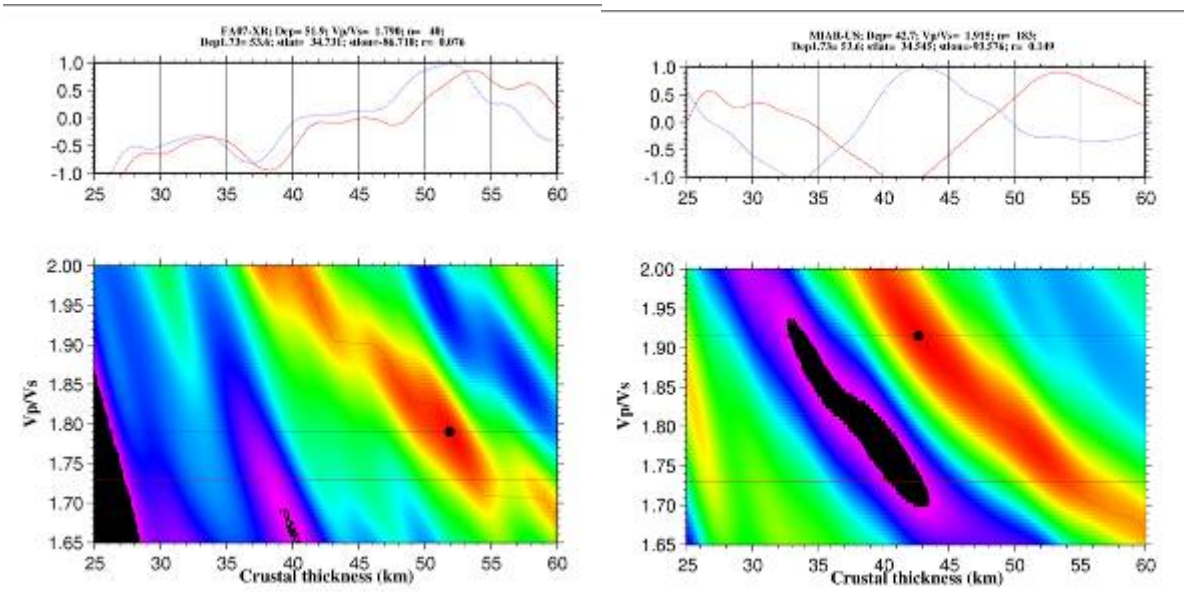

Fig. 6-H-Φ plots for FA07 and MIAR. The red line shows the stacking amplitude for Φ=1.73. The blue line was obtained by using the optimal Φ. The resulting thickness, Φ, and the crustal thickness when Φ=1.73 (denoted as Depth1.73) are shown on the top panels.

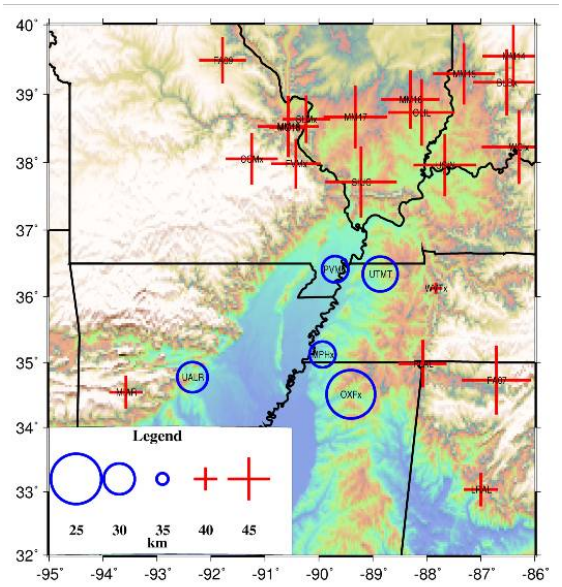

Fig. 7-Resulting crustal thickness (H). Open circles represent stations with a smaller thickness and pluses represents stations with a larger thickness.

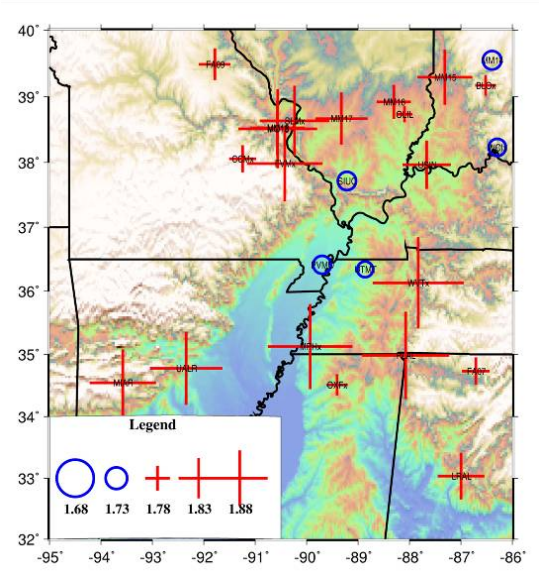

Fig. 8-Resulting crustal Vp/Vs (Φ) for all stations in the study area.

Copyright © 2010, Bioinfo Publications

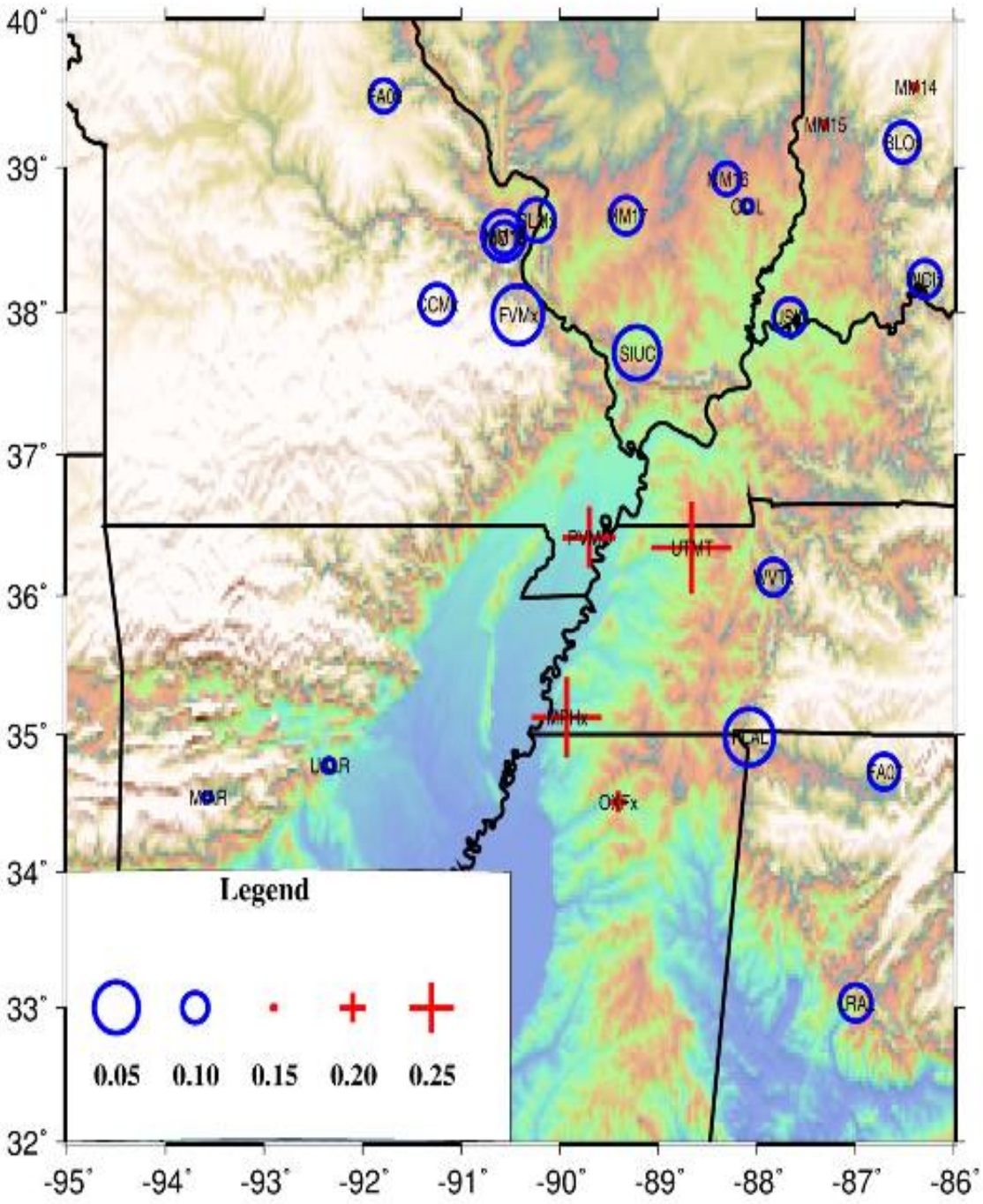

Fig. 9-Resulting ratio (R) of the stacking amplitude corresponding to the optimal pair of (H,Φ) over that of direct P-wave on the radial component. R is calculated for all the stations

Table 1- Observation of Crustal thickness (H,Hn), Vp/Vs(Φ) and Moho sharpness (R).

station	long, deg,	lat, deg,	H, km	Φ	H_n, km	ΔH	ΔΦ	ΔH_n	R	∆R	N^{rfs}	Q
Zone 1												
MPHx	-89.932	35.123	31.3	1.974	43.8	0.1	0.005	0.16	0.319	0.007	170	A
PVMO	-89.7	36.414	31.2	1.742	31.5	0.13	0.008	0	0.274	0.006	161	A
WVTx	-87.83	36.13	36.9	1.995	52.5	0.14	0.001	1.43	0.086	0.003	312	A
OXFx	-89.409	34.512	25.5	1.769	26.8	1.09	0.033	0.25	0.18	0.006	221	A
PLAL	-88.075	34.982	46.3	1.982	37.3	0.12	0.006	4.36	0.038	0.003	223	A
UTMT	-88.864	36.342	29	1.749	29.5	0.15	0.004	0.07	0.348	0.011	130	A
Zone 2												
BLOx	-86.522	39.172	51.1	1.767	52.2	0.15	0.005	0.15	0.077	0.005	187	A
CCMx	-91.245	38.056	47.4	1.788	49.2	0.14	0.003	0.17	0.078	0.002	690	A
SLMx	-90.236	38.636	46.3	1.926	59.8	0.2	0.002	0.01	0.071	0.002	337	A
FVMx	-90.426	37.984	46.8	1.945	53.2	0.35	0.007	8.49	0.034	0.002	210	A
SIUC	-89.217	37.715	52.4	1.741	52.7	1.38	0.016	0.24	0.046	0.002	420	A
USIN	-87.666	37.965	50.1	1.856	58.7	0.21	0.002	0.29	0.084	0.004	207	A
OLIL	-88.099	38.734	51.2	1.752	52.3	0.42	0.006	0.24	0.141	0.006	112	A
FA09	-91.786	39.489	46	1.802	50.2	4.72	0.079	0.25	0.094	0.028	15	A
MM14	-86.395	39.549	50	1.74	50.2	1.24	0.056	0.24	0.154	0.012	29	A
MM15	-87.313	39.295	49.9	1.878	59.8	0.76	0.016	0.05	0.157	0.023	13	A
MM16	-88.305	38.922	49	1.81	51.7	0.31	0.013	1.41	0.096	0.011	44	A
MM17	-89.326	38.669	50.3	1.869	59.1	2.2	0.037	1.59	0.084	0.008	50	A
MM18	-90.569	38.529	49.8	1.877	58.6	1.8	0.025	1.61	0.054	0.007	43	A
MO18	-90.564	38.514	43.8	1.955	57.8	2.65	0.05	0.46	0.094	0.011	11	A
WCIx	-86.294	38.229	53.1	1.744	53.8	0.29	0.006	0.16	0.083	0.005	127	A
UALR	-92.344	34.775	30.2	1.935	38.6	0.14	0.008	0.24	0.138	0.007	173	A
Zone 3												
FA07	-86.71	34.731	51.8	1.789	53.6	0.52	0.015	0.33	0.088	0.01	40	A
LRAL	-86.998	33.035	42.7	1.851	46.9	2.66	0.048	1.2	0.085	0.017	34	A
MIAR	-93.576	34.545	42.6	1.915	53.9	0.44	0.012	0.43	0.148	0.005	183	A

N^{rfs} is the number of receiver function used for calculating H and V_p/V_s
R is the ratio amplitude of the Direct P and its converted phase
Q is the category of quality of H- Φ plots

Copyright © 2010, Bioinfo Publications

Geoscience Research, ISSN: 0976–9846 & E-ISSN: 0976–9854, Vol. 1, Issue 1, 2010